

Analysis on cavitation erosion resistance of isostatic graphite

Ding Hongqin Jiang Shuyun

(School of Mechanical Engineering, Southeast University, Nanjing 211189, China)

Abstract: Isostatic graphite materials with 8% porosity and 14% porosity were prepared by the cold isostatic pressing process. Cavitation erosion resistance of the isostatic graphite was evaluated through cavitation tests in an ultrasonic vibration system. The volume loss and erosion morphology of the isostatic graphite were adopted to investigate the cavitation erosion resistance of the isostatic graphite. The cavitation test results show that after ultrasonic vibration of 14 h, the volume loss of the isostatic graphite materials with 8% porosity and 14% porosity are 35% and 46% of the carbon graphite material, respectively. The isostatic graphite material with 8% porosity exhibits an outstanding capability to resist cavitation erosion damage, and the cavitation erosion resistance of the isostatic graphite enhances with the decrease in porosity. The damage mechanism of isostatic graphite is brittle fracture attributed to the shock wave and micro jet. The isostatic graphite with low porosity exhibits excellent cavitation erosion resistance due to its fine graphite particles, homogeneous structure and high degree of hardness.

Key words: isostatic graphite; cavitation erosion; erosive wear; porosity

DOI: 10.3969/j.issn.1003-7985.2020.02.001

Cavitation is initiated by a local pressure decrease below the level of the saturated vapor pressure in an aqueous environment^[1-4]. The formation and collapse of evaporated cavitation bubbles generate a high micro-jet and shock wave to cause cavitation erosion damage and destroy the material surface^[5-7]. The cavitation erosion phenomenon often occurs in machine components under an aqueous medium, such as large marine propellers, hydrofoils, turbines, pumps and bearings, and it can seriously affect the surface and shorten the service life. Therefore, it is very important to prepare appropriate material with an excellent capability to mitigate the cavitation damage in aqueous environments.

Due to its good self-lubrication properties, corrosion resistance and temperature resistance, graphite material is

potentially suitable for application in water environments^[8-9]. Recently, many researchers have studied the preparation technology, friction and wear properties of graphite material according to various application environments^[10-23]. The tribological test of carbon graphite against metal surface shows that the transferred film depends on pressure, sliding speed and nature of mating surface. The wear rate of carbon graphite is high on the initial sliding and it produces amount of copious carbon debris. Carbon debris is compacted on the counterface. The graphite suffers abrasive rapid wear on the initial sliding stages, which results in the formation of transferred film. The research results show that wear debris are formed in the contact face. After repeated deformation and brittle fracture, the wear particles agglomerate on the wear surfaces. The wear of graphite material is more sensitive to the sliding speed. In addition, the low friction coefficient is attributed to the fluid hydration layers attached to the substrate. In conclusion, the tribological performance of graphite material depends on the process parameters and structure parameters. As a new type of graphite material, isostatic graphite is prepared by the cold isostatic pressing technique^[24-29]. The isostatic graphite is well known for its excellent properties, such as good self-lubrication, low particle size, low open porosity, a homogeneous structure, isotropic properties, a high degree of hardness and strength. The isostatic graphite has a potential application for the high speed water lubricated bearing. The compressive strength range of the high speed water lubricated bearing corresponds to the porosity parameter. Therefore, it is extremely important to study the cavitation erosion behavior of the isostatic graphite material. However, to the best of our knowledge, there is no literature concerned with the cavitation erosion behavior of isostatic graphite material.

In this study, the cavitation erosion behavior of the isostatic graphite was evaluated by an ultrasonic vibratory cavitation experimental facility. The volume loss and erosion morphologies were adopted to illustrate the cavitation erosion behavior of the isostatic graphite. In addition, the cavitation behavior of the carbon graphite was also carried out under the same test conditions for a comparison with the isostatic graphite. This technical note aims to provide fundamental data for the potential application of the isostatic graphite in the aqueous environments.

Received 2019-12-21, **Revised** 2020-04-10.

Biographies: Ding Hongqin (1986—), male, doctor; Jiang Shuyun (corresponding author), male, doctor, professor, jiangshy@seu.edu.cn.

Foundation item: The National Natural Science Foundation of China (No. 51635004, 11472078).

Citation: Ding Hongqin, Jiang Shuyun. Analysis on cavitation erosion resistance of isostatic graphite[J]. Journal of Southeast University (English Edition), 2020, 36 (2): 123 – 127. DOI: 10.3969/j.issn.1003-7985.2020.02.001.

1 Cavitation Erosion Test

1.1 Test specimens

The isostatic graphite materials with 14% porosity and 8% porosity are prepared by the cold isostatic pressing process based on the compressive strength range of the high speed water lubricated bearing. The isostatic graphite materials with 14% porosity and 8% porosity are chosen to study the effect of porosity on the cavitation erosion resistance. The specimen dimension is 10 mm × 5 mm × 7 mm. In addition, the carbon graphite material was also tested for a comparison with the isostatic graphite materials. Fig. 1 shows the specimens of the isostatic graphite and the carbon graphite.

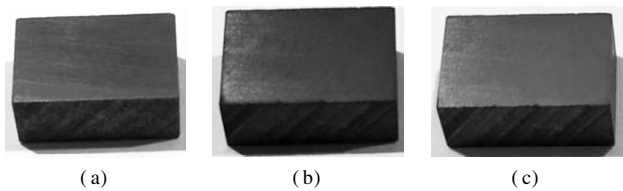


Fig. 1 Specimens of graphite materials. (a) Isostatic graphite with 14% porosity; (b) Isostatic graphite with 8% porosity; (c) Carbon graphite

The microstructure of the as-prepared samples are provided in Fig. 2. Fig. 3 shows the X-ray diffraction pattern of the isostatic graphite. Diffraction peaks of the isostatic graphite appear as hexagonal graphite (2H crystal structure) and rhombohedral graphite (3R crystal structure). The physical parameters of the isostatic graphite and the carbon graphite are listed in Tab. 1. As expected, the

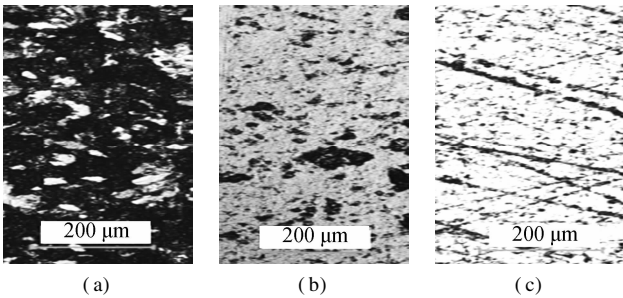


Fig. 2 The microstructure of the as-prepared samples. (a) Carbon graphite; (b) Isostatic graphite with 14% porosity; (c) Isostatic graphite with 8% porosity

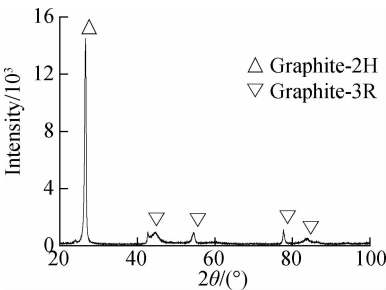


Fig. 3 X-ray diffraction pattern of the isostatic graphite

Tab. 1 Physical parameters of the graphite materials

Parameters	Carbon graphite	Isostatic graphite with 14% porosity	Isostatic graphite with 8% porosity
Bulk density/(g · cm ⁻³)	1.675	1.841	1.936
Shore hardness	40	68	88
Graphite particle size/μm	40	22	3
Open porosity/%	18	14	8
Compressive strength/MPa	75	87	188
Flexural strength/MPa	35	36	81

parameters of the isostatic graphite including density, hardness, strength are greater than those of the carbon graphite. For the isostatic graphite, with the decrease in the average particle size, the porosity decreases, while the volume density, shore hardness, compressive strength and flexural strength increase.

1.2 Cavitation test

An ultrasonic vibration system was used to study the cavitation erosion behavior of the isostatic graphite, as shown in Fig. 4. The ultrasonic vibration system was driven by an ultrasound generator at a frequency of 20 kHz and an amplitude of 6 μm. The ASTM G32 standard

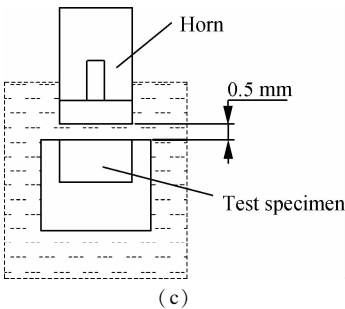
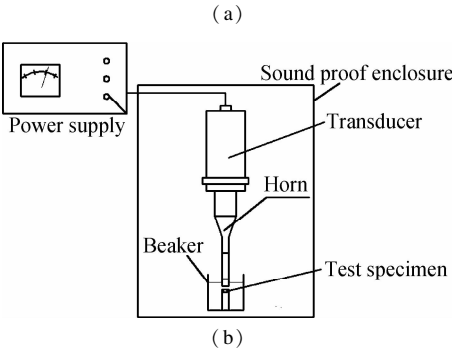
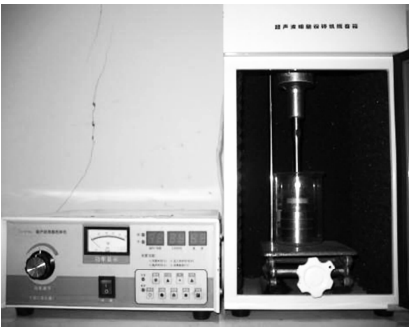


Fig. 4 The ultrasonic vibration system. (a) Real scene image; (b) Schematic diagram; (c) Specimen holder

was adopted to assess the cavitation erosion behavior of the isostatic graphite^[30]. The separation distance between the ultrasonic horn tip and the sample was 0.5 mm. The distance between the liquid level and the horn tip was 15 mm. The counterpart material in the cavitation tests was stainless steel. The specimen was attached to the specimen holder facing the horn tip. Tap water was used as the test liquid. The tap water was changed every 30 min to maintain the temperature of the tap water at $(20 \pm 2)^\circ\text{C}$ in the beaker.

1.3 Test procedures

The cavitation erosion behavior of the isostatic graphite is evaluated by an ultrasonic vibration system. The cavitation experiment is performed with a duration of 14 h for each specimen. The specimens are weighed, cleaned and dried in turn. Subsequently, the specimens are weighed with a high-precision scale (the accuracy of 0.01 mg) before and after each cavitation test. The test results of the three experiments are averaged, including the standard deviation. The graphite specimens after the cavitation experiments are given in Fig. 5.

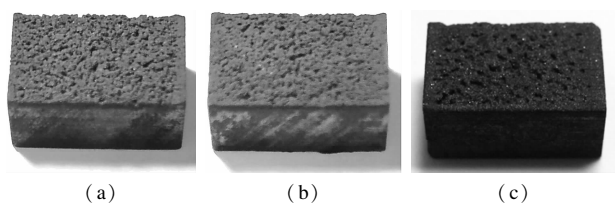


Fig. 5 Graphite specimens after cavitation tests. (a) Isostatic graphite with 14% porosity; (b) Isostatic graphite with 8% porosity; (c) Carbon graphite

2 Results and Discussion

2.1 Volume loss

Fig. 6 shows the volume loss curves of the carbon graphite and the isostatic graphite after cavitation tests in tap water. The results show that the volume loss of the graphite specimen increases with the test time, and the isostatic graphite exhibits better cavitation erosion resistance in comparison with the carbon graphite. The cavitation

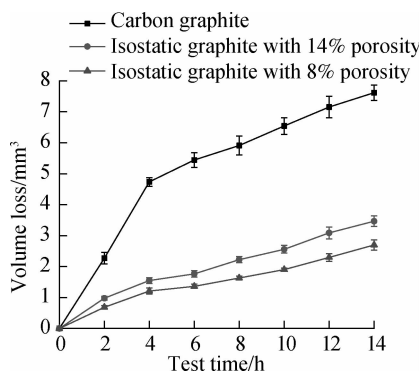


Fig. 6 The volume loss curves of the isostatic graphite and carbon graphite after the cavitation test

erosion resistance of the isostatic graphite increases with the decrease in the porosity. After a cavitation test of 14 h, the volume loss of the carbon graphite, the isostatic graphite with 14% porosity and the isostatic graphite with 8% porosity are 7.61, 3.47 and 2.70 mm³, respectively. The main reason is that the isostatic graphite with 8% porosity represents excellent mechanical properties (such as a high degree of shore hardness) compared with the carbon graphite and isostatic graphite with 14% porosity.

2.2 Erosion morphology

Fig. 7 shows the scanning electron microscope (SEM) images of the carbon graphite and the isostatic graphite after a cavitation test of 14 h. It can be seen that the cavitation erosion damage occurs on the surfaces of the two materials. The surface of the graphite is attacked by cavitation bubbles breakup, and then the micro jet and shock wave lead to the formation of pits and craters on the sample surface due to the porosity and inherent brittleness of the materials. With the duration of the test, the repeated impact due to cavitation bubbles breakup will

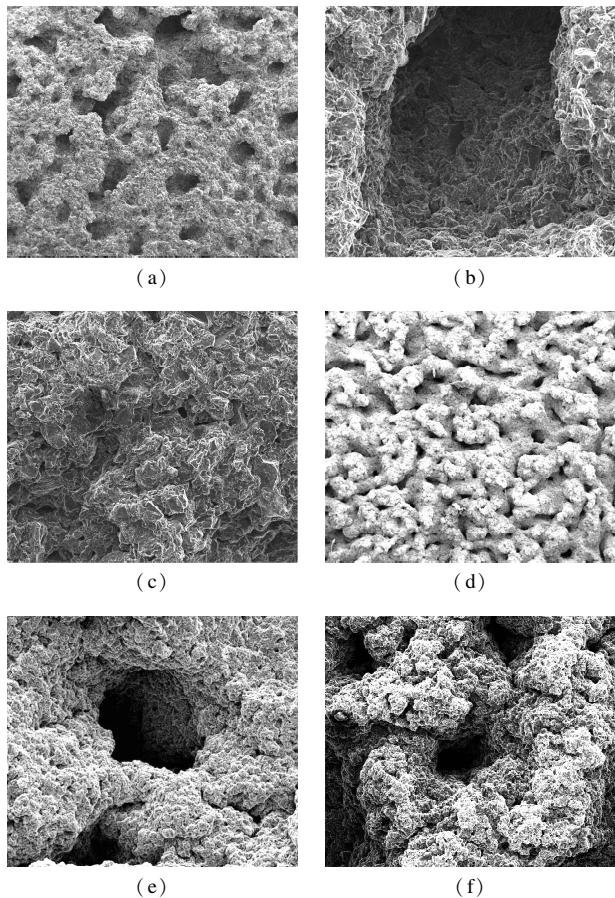


Fig. 7 SEM images of graphite materials after a cavitation test of 14 h. (a) Carbon graphite in low magnification; (b) A large pit of carbon graphite in high magnification; (c) Weak damage area of carbon graphite; (d) Isostatic graphite with 8% porosity in low magnification; (e) A large pit of isostatic graphite with 14% porosity in high magnification; (f) A small pit of isostatic graphite with 8% porosity in high magnification

cause continuous material spalling of the graphite surface by brittle fracture.

It is particularly visible from Figs. 7 (a) to (c) that large pits and deep craters appear on the eroded surface and the cavitation erosion damage of the carbon graphite sample is very serious. A possible explanation might be that the carbon graphite material has a low degree of hardness, is brittle and has a high open-cell porosity. When the carbon graphite material is attacked by the cavitation bubbles breakup, the erosion pits will form on the surface. Large pits and deep craters are aggregated and consolidated during the cavitation test.

On the contrary, as shown in Figs. 7 (d) and (f), small erosion pits are observed on the surfaces of the isostatic graphite after the cavitation tests. This result may be explained by the fact that the isostatic graphite has an excellent physical properties such as homogeneous structure, uniform physicochemical properties and isotropy, low open-cell porosity, a high degree of hardness and compressive strength. All those are beneficial to resist the shock wave and micro jet. As a consequence, the cavitation erosion damage degree of the isostatic graphite is not as serious as that in the carbon graphite material. Fig. 8 shows the cavitation erosion mechanism of the isostatic graphite. Many cavitation bubbles impact the graphite surface and lead to the brittle fracture of the isostatic graphite.

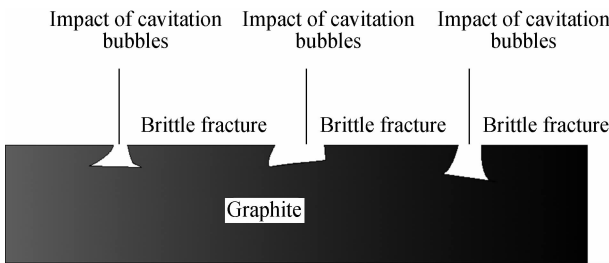


Fig. 8 The erosion mechanism of isostatic graphite

3 Conclusions

1) The isostatic graphite exhibits an outstanding capability to resist cavitation erosion damage compared with the carbon graphite, and the cavitation erosion resistance of the isostatic graphite increases with the decrease in porosity.

2) The excellent cavitation erosion resistance of the isostatic graphite can be attributed to its physical properties, such as a homogeneous structure, a high degree of hardness, a low open-cell porosity, uniform physicochemical properties and isotropy.

3) It is guaranteed that the isostatic graphite is an application for high speed water lubricated bearing.

References

[1] Mitelea I, Ghera C, Bordeasu I, et al. Assessment of

cavitation erosion of gas-nitrided Cr-Ni-Mo steels [J]. *Journal of Tribology*, 2018, **140** (6): 061601-1 – 061601-8. DOI:10.1115/1.4039133.

[2] Abouel-Kasem A, Ahmed S M. Bubble structures between two walls in ultrasonic cavitation erosion [J]. *Journal of Tribology*, 2012, **134** (2): 021702-1 – 021702-9. DOI:10.1115/1.4005217.

[3] Abouel-Kasem A, El-Deen A E, Emara K M, et al. Investigation into cavitation erosion pits [J]. *Journal of Tribology*, 2009, **131** (3): 031605-1 – 031605-7. DOI: 10.1115/1.3075863.

[4] Zhang L, Zhang Y K, Lu J Z, et al. Effects of laser shock processing on electrochemical corrosion resistance of ANSI 304 stainless steel weldments after cavitation erosion [J]. *Corrosion Science*, 2013, **66**: 5 – 13. DOI: 10.1016/j.corsci.2012.08.034.

[5] Abouel-Kasem A, Ahmed S M. Cavitation erosion mechanism based on analysis of erosion particles [J]. *Journal of Tribology*, 2008, **130** (3): 031601-1 – 031601-6. DOI:10.1115/1.2913552.

[6] Jiang S Y, Ding H Q, Xu J. Cavitation erosion resistance of sputter-deposited Cr₃Si film on stainless steel [J]. *Journal of Tribology*, 2017, **139** (1): 014501-1 – 014501-5. DOI:10.1115/1.4033049.

[7] Ding H Q, Jiang S Y. Cavitation erosion resistance of silicified graphite by liquid silicon penetration technique [J]. *Journal of Tribology*, 2017, **139** (6): 064501-1 – 064501-5. DOI:10.1115/1.4035869.

[8] Jia Q, Yuan X Y, Zhang G Y, et al. Dry friction and wear characteristics of impregnated graphite in a corrosive environment [J]. *Chinese Journal of Mechanical Engineering*, 2014, **27** (5): 965 – 971. DOI:10.3901/cjme.2014.0616.111.

[9] Jones G. On the tribological behaviour of mechanical seal face materials in dry line contact [J]. *Wear*, 2004, **256** (3/4): 415 – 432. DOI: 10.1016/s0043-1648 (03) 00539-8.

[10] Batchelor A W, Lam L N, Chandrasekaran M. Lubrication of stellite at ambient and elevated temperatures by transfer films from a graphite slider [J]. *Wear*, 1996, **198** (1/2): 208 – 215. DOI:10.1016/0043-1648(96)06967-0.

[11] Williams J A, Morris J H, Ball A. The effect of transfer layers on the surface contact and wear of carbon-graphite materials [J]. *Tribology International*, 1997, **30** (9): 663 – 676. DOI:10.1016/s0301-679x(97)00034-0.

[12] Cui G J, Bi Q L, Yang J, et al. Effect of normal loads on tribological properties of bronze-graphite composite under seawater condition [J]. *Tribology Transactions*, 2014, **57** (2): 308 – 316. DOI: 10.1080/10402004.2013.877177.

[13] Zhu Z G, Bai S, Wu J F, et al. Friction and wear behavior of resin/graphite composite under dry sliding [J]. *Journal of Materials Science & Technology*, 2015, **31** (3): 325 – 330. DOI:10.1016/j.jmst.2014.10.004.

[14] Zhang G L, Liu Y, Guo F, et al. Friction characteristics of impregnated and non-impregnated graphite against cemented carbide under water lubrication [J]. *Journal of Materials Science & Technology*, 2017, **33** (10): 1203 – 1209. DOI:10.1016/j.jmst.2016.06.013.

- [15] Kováčik J, Emmer Š, Bielek J, et al. Effect of composition on friction coefficient of Cu-graphite composites[J]. *Wear*, 2008, **265** (3/4): 417 – 421. DOI:10.1016/j.wear.2007.11.012.
- [16] Liu Y B, Lim S C, Ray S, et al. Friction and wear of aluminium-graphite composites: The smearing process of graphite during sliding[J]. *Wear*, 1992, **159** (2): 201 – 205. DOI:10.1016/0043-1648(92)90303-p.
- [17] Rajkumar K, Aravindan S. Microwave sintering of copper-graphite composites[J]. *Journal of Materials Processing Technology*, 2009, **209** (15/16): 5601 – 5605. DOI:10.1016/j.jmatprotec.2009.05.017.
- [18] Rajkumar K, Kundu K, Aravindan S, et al. Accelerated wear testing for evaluating the life characteristics of copper-graphite tribological composite[J]. *Materials & Design*, 2011, **32** (5): 3029 – 3035. DOI:10.1016/j.matdes.2011.01.046.
- [19] Ma W L, Lu J J. Effect of sliding speed on surface modification and tribological behavior of copper-graphite composite[J]. *Tribology Letters*, 2011, **41** (2): 363 – 370. DOI:10.1007/s11249-010-9718-x.
- [20] Gulevskii V A, Antipov V I, Kolmakov A G, et al. Designing of copper-based alloys for the impregnation of carbon-graphite materials[J]. *Russian Metallurgy (Metally)*, 2012, **2012** (3): 258 – 261. DOI:10.1134/s0036029512030081.
- [21] Hirani H, Goilkar S S. Formation of transfer layer and its effect on friction and wear of carbon-graphite face seal under dry, water and steam environments[J]. *Wear*, 2009, **266** (11/12): 1141 – 1154. DOI:10.1016/j.wear.2009.03.018.
- [22] Serre I, Celati N, Pradeilles-Duval R. Tribological and corrosion wear of graphite ring against $\text{Ti}_6\text{Al}_4\text{V}$ disk in artificial sea water[J]. *Wear*, 2002, **252** (9/10): 711 – 718. DOI:10.1016/s0043-1648(02)00030-3.
- [23] Cui G J, Bi Q L, Zhu S Y, et al. Tribological properties of bronze-graphite composites under sea water condition[J]. *Tribology International*, 2012, **53**: 76 – 86. DOI:10.1016/j.triboint.2012.04.023.
- [24] Salavati H, Alizadeh Y, Ayatollahi M R. Fracture assessment of inclined double keyhole notches in isostatic graphite[J]. *Physical Mesomechanics*, 2018, **21** (2): 110 – 116. DOI:10.1134/s1029959918020030.
- [25] Torabi A R. Sudden fracture from U-notches in fine-grained isostatic graphite under mixed mode I/II loading[J]. *International Journal of Fracture*, 2013, **181** (2): 309 – 316. DOI:10.1007/s10704-013-9832-5.
- [26] Berto F, Lazzarin P, Ayatollahi M R. Brittle fracture of sharp and blunt V-notches in isostatic graphite under torsion loading[J]. *Carbon*, 2012, **50** (5): 1942 – 1952. DOI:10.1016/j.carbon.2011.12.045.
- [27] Berto F, Lazzarin P, Ayatollahi M R. Brittle fracture of sharp and blunt V-notches in isostatic graphite under pure compression loading[J]. *Carbon*, 2013, **63**: 101 – 116. DOI:10.1016/j.carbon.2013.06.045.
- [28] Lazzarin P, Berto F, Ayatollahi M R. Brittle failure of inclined key-hole notches in isostatic graphite under in-plane mixed mode loading[J]. *Fatigue & Fracture of Engineering Materials & Structures*, 2013, **36** (9): 942 – 955. DOI:10.1111/ffe.12057.
- [29] Berto F, Lazzarin P, Marangon C. Brittle fracture of U-notched graphite plates under mixed mode loading[J]. *Materials & Design*, 2012, **41**: 421 – 432. DOI:10.1016/j.matdes.2012.05.022.
- [30] ASTM G32-16. Standard test method for cavitation erosion using vibratory apparatus[S]. West Conshohocken, PA, USA: ASTM International, 2016.

等静压石墨抗空蚀性能分析

丁红钦 蒋书运

(东南大学机械工程学院, 南京 211189)

摘要:通过冷等静压工艺制备了孔隙率为8%和14%的等静压石墨,通过超声振动空蚀试验系统对等静压石墨的抗空蚀性能进行了研究,采用等静压石墨的体积损失和表面破坏形貌揭示其抗空蚀性能.空蚀试验结果表明:超声振动14 h后,与普通碳石墨相比,孔隙率为8%和14%的等静压石墨体积损失分别为普通碳石墨的35%和46%;孔隙率为8%的等静压石墨表现出更强的抗空蚀能力,且等静压石墨的抗空蚀能力随着孔隙率的降低而增加;等静压石墨空蚀破坏的机制是冲击波和微射流作用下等静压石墨材料的脆性断裂;由于粒度小、组织均匀及硬度高,低孔隙率的等静压石墨表现出良好抗空蚀性能.

关键词:等静压石墨;空蚀;冲蚀磨损;孔隙

中图分类号:TH117